A&A 634, C2 (2020)
https://doi.org/10.1051/0004-6361/201935679e

Astronomy & Astrophysics

The CARMENES search for exoplanets around M dwarfs

Photospheric parameters of target stars from high-resolution spectroscopy. II. Simultaneous multi-wavelength range modeling of activity insensitive lines *(Corrigendum)*

V. M. Passegger[1], A. Schweitzer[1], D. Shulyak[2], E. Nagel[1], P. H. Hauschildt[1], A. Reiners[3], P. J. Amado[4], J. A. Caballero[5], M. Cortés-Contreras[5], A. J. Domínguez-Fernández[6], A. Quirrenbach[7], I. Ribas[8,9], M. Azzaro[10], G. Anglada-Escudé[4,11], F. F. Bauer[4], V. J. S. Béjar[12,13], S. Dreizler[3], E. W. Guenther[14], T. Henning[15], S. V. Jeffers[3], A. Kaminski[7], M. Kürster[15], M. Lafarga[8,9], E. L. Martín[5], D. Montes[6], J. C. Morales[8,9], J. H. M. M. Schmitt[1], and M. Zechmeister[3]

[1] Hamburger Sternwarte, Gojenbergsweg 112, 21029 Hamburg, Germany
e-mail: vpassegger@hs.uni-hamburg.de
[2] Max Planck Institute for Solar System Research, Justus-von-Liebig-Weg 3, 37077 Göttingen, Germany
[3] Institut für Astrophysik, Georg-August-Universität, Friedrich-Hund-Platz 1, 37077 Göttingen, Germany
[4] Instituto de Astrofísica de Andalucía (IAA-CSIC), Glorieta de la Astronomía s/n, 18008 Granada, Spain
[5] Centro de Astrobiología (CSIC-INTA), ESAC, Camino Bajo del Castillo s/n, 28692 Villanueva de la Cañada, Madrid, Spain
[6] Departamento de Física de la Tierra y Astrofísica and IPARCOS-UCM (Instituto de Física de Partículas y del Cosmos de la UCM), Facultad de Ciencias Físicas, Universidad Complutense de Madrid, 28040 Madrid, Spain
[7] Landessternwarte, Zentrum für Astronomie der Universtät Heidelberg, Königstuhl 12, 69117 Heidelberg, Germany
[8] Institut de Ciències de l'Espai (CSIC-IEEC), Campus UAB, c/ de Can Magrans s/n, 08193 Bellaterra, Barcelona, Spain
[9] Institut d'Estudis Espacials de Catalunya (IEEC), 08034 Barcelona, Spain
[10] Centro Astronómico Hispano-Alemán (CSIC-MPG), Observatorio Astronómico de Calar Alto, Sierra de los Filabres, 04550 Gérgal, Almería, Spain
[11] School of Physics and Astronomy, Queen Mary, University of London, 327 Mile End Road, London, E1 4NS, UK
[12] Instituto de Astrofísica de Canarias, c/ Vía Láctea s/n, 38205 La Laguna, Tenerife, Spain
[13] Departamento de Astrofísica, Universidad de La Laguna, 38206 La Laguna, Tenerife, Spain
[14] Thüringer Landessternwarte Tautenburg, Sternwarte 5, 07778 Tautenburg, Germany
[15] Max-Planck-Institut für Astronomie, Königstuhl 17, 69117 Heidelberg, Germany

A&A, 627, A161 (2019), https://doi.org/10.1051/0004-6361/201935679

Key words. astronomical databases: miscellaneous – methods: data analysis – techniques: spectroscopic – stars: late-type – stars: fundamental parameters – errata, addenda

We have corrected an error in Passegger et al. (2019) in the calculation of the stellar surface gravity $\log g$ from literature masses and radii provided by Gaidos & Mann (2014) and Mann et al. (2015). The mass and radius were interchanged in the formula, $g = GM/R^2$ which resulted into too high $\log g$ values for the earliest M dwarfs. This mistake only affected the part where our $\log g$ values were compared to literature values and had no influence on our parameters which had been derived from high-resolution spectra. In the framework of this corrigendum, we also correct a few other minor mistakes and typos. In the following, we describe all changes in detail.

Section 4.2. We replot Figs. 5–7, where only the middle panel presenting $\log g$ has changed for literature values from Gaidos & Mann (2014) and Mann et al. (2015). In the second paragraph, line 8, sentences 6 and 7 should read:

"For $\log g$ we find a good correlation with the literature, although a small offset towards lower values can be seen for our results. For this parameter as well as for metallicity, results from Raj18 do not correlate with our values nor with the other literature, spreading across the whole parameter range."

We recalculate the mean absolute difference between our results and literature in Table 3 after correcting the error in the aforementioned $\log g$ calculation from masses and radii published by Mann et al. (2015) and Gaidos & Mann (2014). This leads to a decrease of MADs in $\log g$ for all wavelength ranges. Additionally, we correct a minor typo in the MAD calculation for Rajpurohit et al. (2018) and Schweitzer et al. (2019), which leads to differences of less than 1 K and less than 0.05 dex in the single and total MADs. In the last paragraph, line 6, sentences 5 and 6 should read:

"For $\log g$ and metallicity, the MADs are mostly within our errorbars for VIS+NIR and VIS."

Section 4.3. Our description of the definition of active stars in Fig. 8 was not accurate, as it actually showed only stars with both Hα pseudo-equivalent width less than –0.3 Å and Ca II emission. To match the description in the text, we also include stars that only show Ca II emission alone. Therefore, we correct Fig. 8 regarding $\log g$ (middle panel) and activity (all panels), which results in a reduction of outliers. In the first paragraph, line 1, sentence 1 and line 7, sentence 5 should read:

"In the following we will discuss some outliers from Fig. 7, mainly considering metallicity. (...) Stars showing Ca II emission are identified in Table B.1 with an activity flag 1."

In the second paragraph, line 4, sentence 4 should read:

"Most of these stars are active. However, they correspond well to literature values within their errors, which supports our method of line selection since we found this parameter to be most influenced by activity."

In the third paragraph, line 8, sentences 5, 6, and 7 should read:

"In $\log g$, we find them at both ends of the plot at low and high values."

Outliers (6) and (7) in $\log g$ disappear due to the correction of the derived literature value. Outliers (9) and (11) in temperature show Ca II emission and are now considered as active. This results in the following renumbering of outliers after (5) J17578+046 (Barnard's star). The discussion for each outlier remains unchanged.

(6) J22115+184
(7) J02222+478
(8) J05127+196

The rest of the results and discussion remain unaffected.

Appendix B. There was a typo in Table B.2 for the NIR and VIS parameter values of J23431+365. We update Table B.2 accordingly.

Acknowledgements. We thank Yutong Shan for pointing out this error.

References

Gaidos, E., & Mann, A. W. 2014, ApJ, 791, 54
Maldonado, J., Affer, L., Micela, G., et al. 2015, A&A, 577, A132
Mann, A. W., Feiden, G. A., Gaidos, E., Boyajian, T., & von Braun, K. 2015, ApJ, 804, 64
Passegger, V. M., Schweitzer, A., Shulyak, D., et al. 2019, A&A, 627, A161
Rajpurohit, A. S., Allard, F., Rajpurohit, S., et al. 2018, A&A, 620, A180
Rojas-Ayala, B., Covey, K. R., Muirhead, P. S., & Lloyd, J. P. 2012, ApJ, 748, 93
Schweitzer, A., Passegger, V. M., Cifuentes, C., et al. 2019, A&A, 625, A68

Table 3. Mean absolute difference between literature and results of this work for different wavelength ranges.

Work	VIS+NIR $T_{\rm eff}$ [K]/log g/[Fe/H]	NIR $T_{\rm eff}$ [K]/log g/[Fe/H]	VIS $T_{\rm eff}$ [K]/log g/[Fe/H]
Maldonado et al. (2015)	49.97/0.094/0.212	53.98/0.104/0.262	46.50/0.088/0.184
Rojas-Ayala et al. (2012)	84.02/.../0.152	82.46/.../0.194	82.03/.../0.142
Gaidos & Mann (2014)	68.85/0.07/0.157	57.64/0.089/0.228	72.51/0.064/0.133
Mann et al. (2015)	60.19/0.06/0.152	66.07/0.079/0.226	55.88/0.056/0.136
Rajpurohit et al. (2018)	77.18/0.402/0.248	86.60/0.423/0.289	69.907/0.397/0.246
Schweitzer et al. (2019)	43.98/0.136/0.116	55.45/0.160/0.223	45.56/0.127/0.082
Total	61.76/0.215/0.173	68.93/0.236/0.246	59.52/0.208/0.155
Total (w/o Rajpurohit et al. 2018)	53.80/0.109/0.135	59.77/0.131/0.223	54.16/0.102/0.108

Table B.2. Basic astrophysical parameters of investigated stars for different wavelength regimes.

	VIS+NIR			NIR			VIS		
Karmn	$T_{\rm eff}$	log g	[Fe/H]	$T_{\rm eff}$	log g	[Fe/H]	$T_{\rm eff}$	log g	[Fe/H]
J23431+365	3215 ± 54	4.95 ± 0.06	–0.03 ± 0.19	3215 ± 56	4.94 ± 0.04	–0.01 ± 0.16	3221 ± 51	4.94 ± 0.04	–0.01 ± 0.16

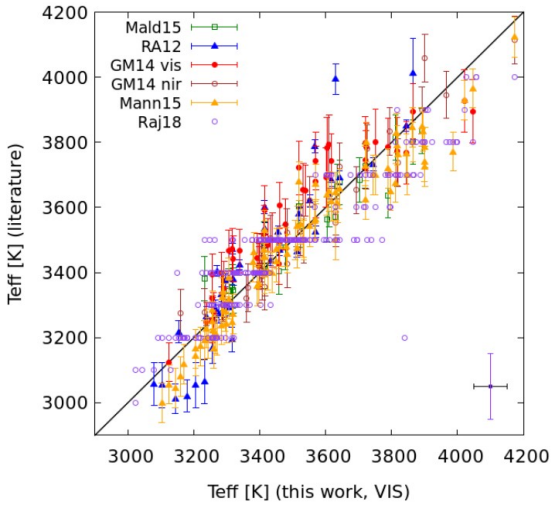

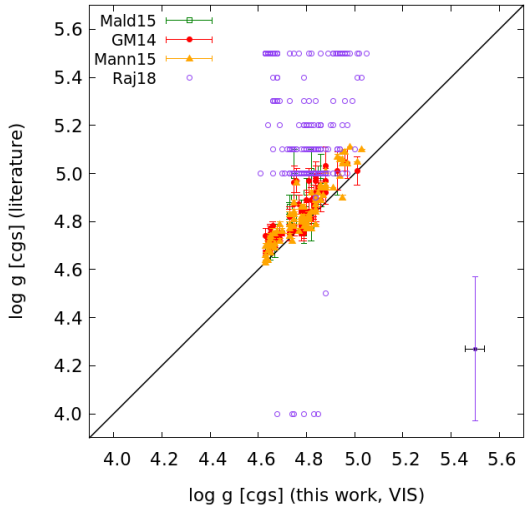

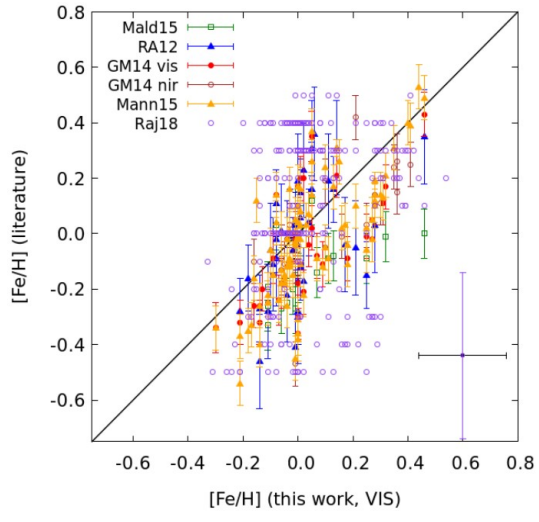

Fig. 5. Comparison between results from VIS and literature values for $T_{\rm eff}$ (*top panel*), $\log g$ (*middle panel*), and [Fe/H] (*bottom panel*). The 1:1 relation is indicated by the black line. The uncertainties of this work (black) are shown in the lower right corner of each panel together with the uncertainties of Rajpurohit et al. (2018) (purple).

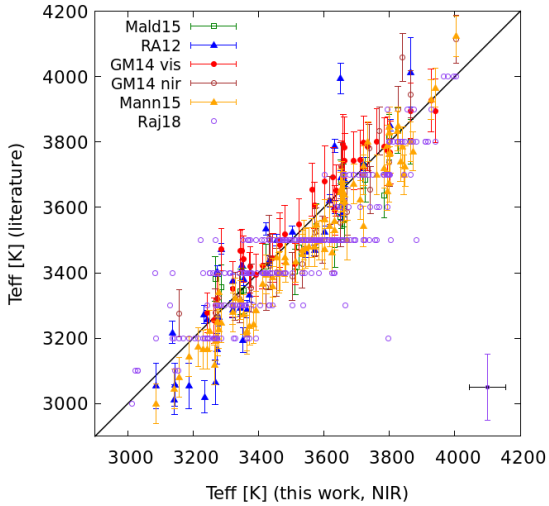

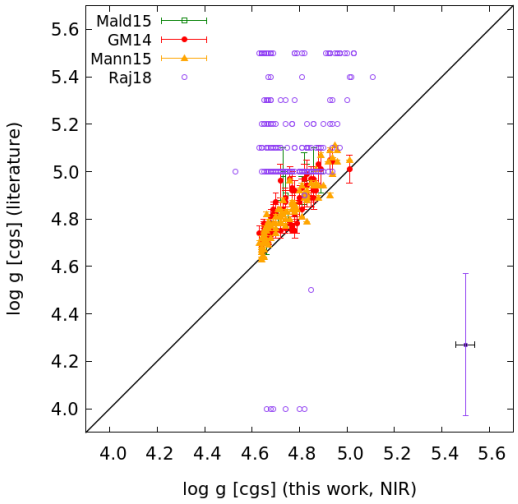

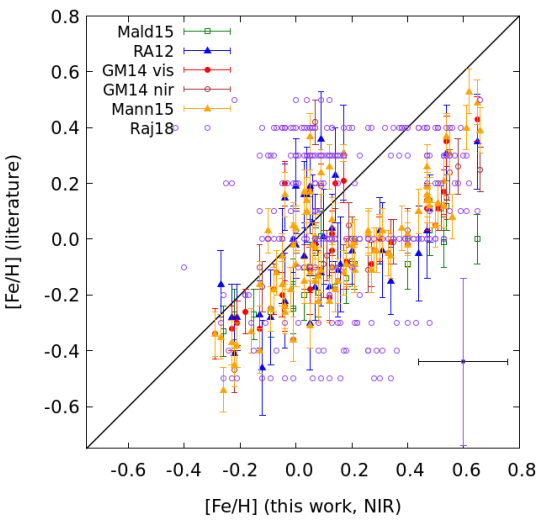

Fig. 6. Comparison between results from the NIR and literature values for $T_{\rm eff}$ (*top panel*), $\log g$ (*middle panel*), and [Fe/H] (*bottom panel*). The 1:1 relation is indicated by the black line. The uncertainties of this work (black) are shown in the lower right corner of each panel together with the uncertainties of Rajpurohit et al. (2018) (purple).

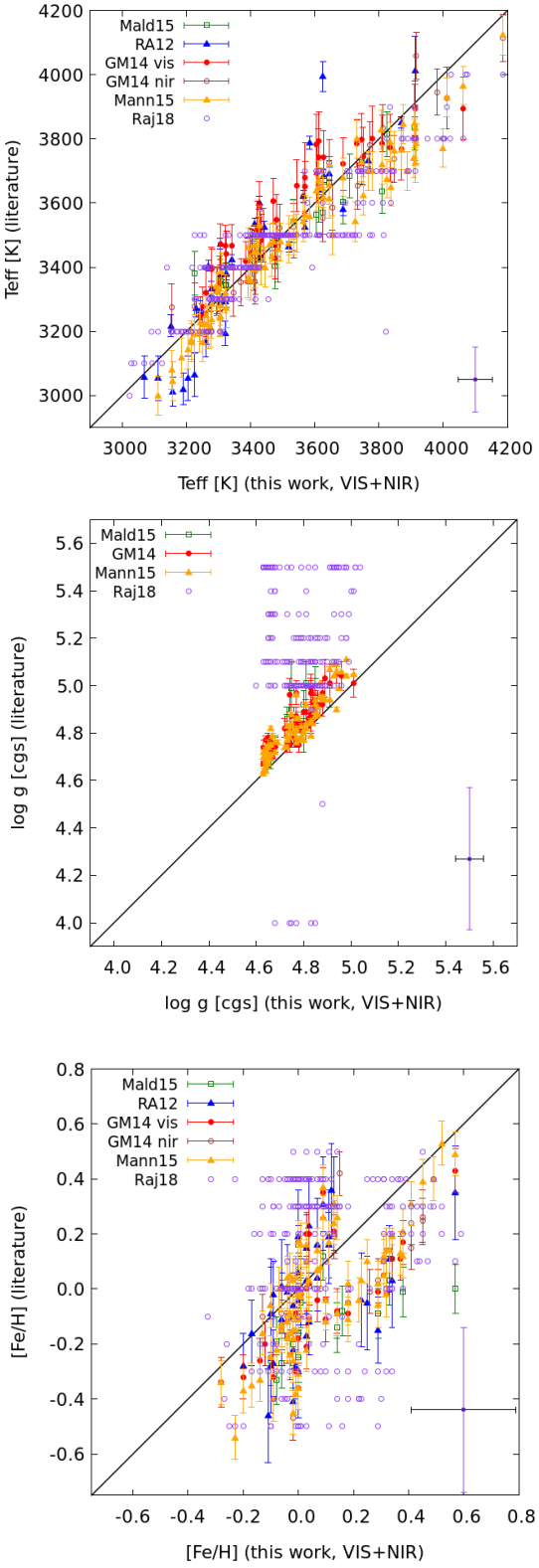

Fig. 7. Comparison between results from VIS+NIR and literature values for $T_{\rm eff}$ (*top panel*), log g (*middle panel*), and [Fe/H] (*bottom panel*). The 1:1 relation is indicated by the black line. The uncertainties of this work (black) are shown in the lower right corner of each panel together with the uncertainties of Rajpurohit et al. (2018) (purple).

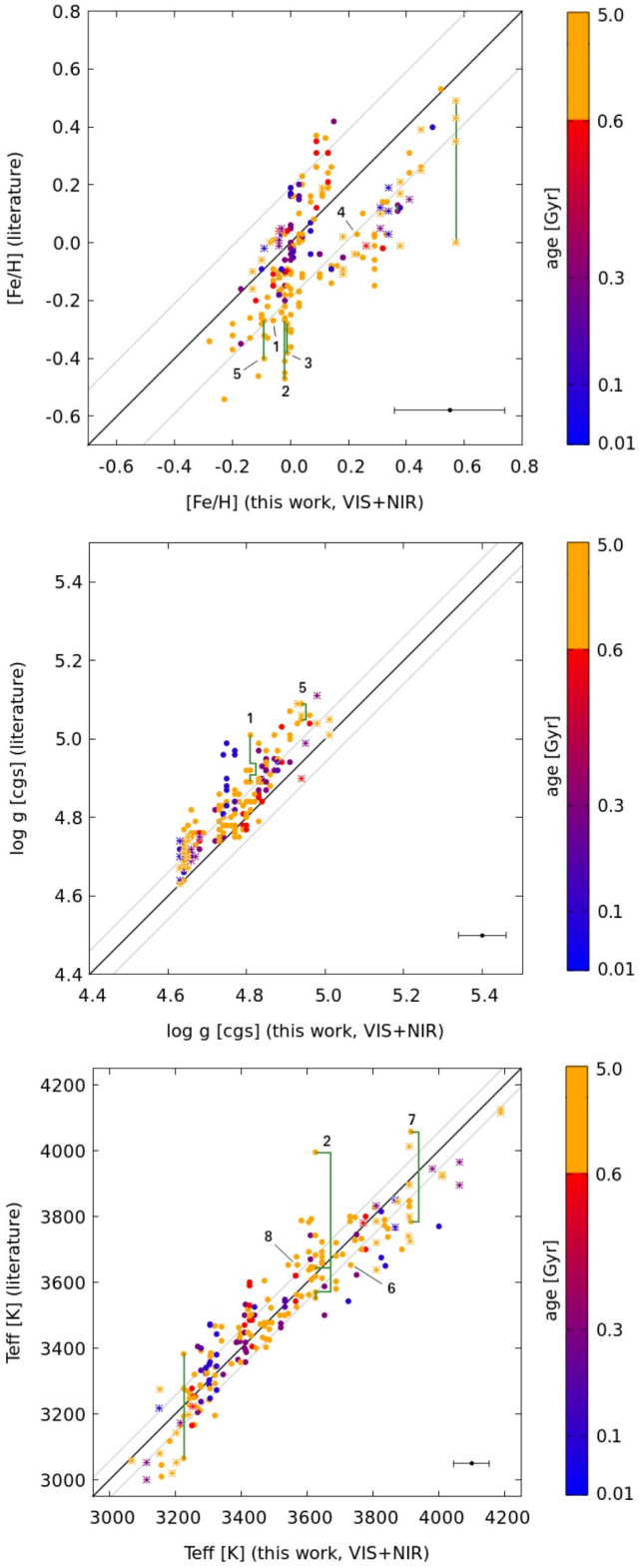

Fig. 8. Comparison of [Fe/H] (*top panel*), log g (*middle panel*), and $T_{\rm eff}$ (*bottom panel*) between values of this work in VIS+NIR and literature. The age is color-coded, active star are plotted as asterisks. Outliers are identified with numbers, the green lines connect different literature values for them. The black line indicates the 1:1 relation, the grey lines the 1σ deviation.